New methods of analyzing indentation experiments on very thin films

Han Li[a], Nicholas X. Randall[b], Joost J. Vlassak[a] *

[a] *School of Engineering and Applied Sciences, Harvard University*

Cambridge, Massachusetts, 02138, USA

[b] *CSM Instruments, Needham, Massachusetts 02494, USA*

Abstract - Indentation experiments on very thin films are analyzed by employing a rigorous solution to model elastic substrate effects. Two cases are discussed: elastic indentations where film and substrate are anisotropic, and elasto-plastic indentations where significant material pile-up occurs. We demonstrate that the elastic modulus of a thin film can be accurately measured in both cases, even if there is significant elastic mismatch between film and substrate.

Keywords: Nano-indentation, Substrate Effect, Thin Films, Elastic properties

*Corresponding author. e-mail: vlassak@esag.harvard.edu

I. INTRODUCTION

In materials research and nanotechnology, instrumented indentation has evolved into a powerful tool for probing the mechanical response of a material at the micro- and nanometer length scales. Applications are widespread, ranging from metals and ceramics to polymers and biomaterials [1-3]. A number of material properties can be deduced from the measured load-displacement (P-h) curve [1-3], although proper interpretation of the experimental results requires an accurate model of how the material interacts with the indenter. Sometimes direct imaging of the indentations may be required as well [4-9].

One problem of technological interest that comes back time and again is how to measure the properties of a very thin film on a substrate using indentation techniques. Substrate effects in indentation experiments are well known, but a robust procedure for evaluating the substrate effect quantitatively and for extracting intrinsic film properties remains elusive. Often indentations are limited to less than 10% of the film thickness to avoid substrate effects. This rule of thumb does not work well, if there is a large elastic mismatch between film and substrate [10, 11] – especially so if the film is stiffer than the substrate [11, 12]. Furthermore, for very thin films the indentation depth required to avoid the substrate effect is so small that it is difficult if not impossible to obtain any meaningful experimental results.

Extensive theoretical and experimental efforts have been devoted to understanding the role of the substrate in modeling the overall contact response and in the interpretation of experimental data [10-21]. A recent review on this subject is given in [22, 23]. Among these efforts, Yu et al solved the axisymmetric contact problem for a layered elastic half-space [16], providing results that generalize Sneddon's well-known equation for a monolithic material [24]. Yu's solution has been employed for analyzing elasto-plastic indentations subject to various restrictions [17, 19].

In this paper, we proceed along this line of development, and revisit two familiar scenarios where Yu's analysis can be applied in a novel and simple way. We begin with a brief review of

Yu's solution and relevant results. Following that, we present (1) an analysis of elastic indentations where the film and/or substrate materials are anisotropic, and (2) an analysis of elasto-plastic indentations where material pile-up around the indenter is significant. We demonstrate that the elastic modulus of the film can be accurately determined even if there is significant elastic mismatch between film and substrate.

II. REVIEW OF YU'S ELASTIC SOLUTION

The axisymmetric indentation of a layered half-space that consists of elastically isotropic and uniform materials is mathematically a mixed boundary value problem that can be reduced to a Fredholm integral equation of the second kind using Papkovich-Neuber potentials [16]:

$$H(\tau) - \frac{1}{\pi}\int_0^1 \left[K(y+\tau) + K(y-\tau) \right] H(y)\,dy = F_0(\tau) \tag{1}$$

The solution of the contact problem is given in terms of a function $H(\tau)$ and a parameter γ. The function $H(\tau)$ can be regarded as a normalized pressure distribution within the contact region, with $\tau = 0$ at the indenter apex and $\tau = 1$ at the contact periphery. $H(\tau)$ must satisfy the boundary condition $H(1) = 0$, which physically means that for a smooth punch the pressure vanishes at the contact periphery. The parameter γ is the ratio of the contact radius for an indentation in a film/substrate composite to the contact radius for an indentation to the same depth in a homogenous medium with the same properties as the film, i.e. $\gamma = a/a^H$. The kernel $K(y)$ of the integral equation is a continuous function that depends on the elastic properties of film and substrate, as well as on the bonding conditions at their interface. For a perfectly bonded interface, an explicit expression of $K(y)$ is given in [16, 17, 19]. The elastic properties of film and substrate enter this expression via their respective plane-strain moduli, M_f and M_s, and via their Poisson's ratios, ν_f and ν_s. The subscript denotes the film and substrate respectively. $F_0(\tau)$ is a dimensionless function determined only by the punch geometry, the explicit expression for which

is given in [16] for conical, spherical and flat-ended punches. The integral equation can be solved numerically for $H(\tau)$ and γ using Elgendi's algorithm [25]. $H(\tau)$ and γ are then used to calculate the indentation load, *P*, and the contact radius, *a*, as functions of the indentation depth, *h* [16, 17, 19]. As the contact stiffness, *S*, is simply the derivative of *P* with respect to *h* for elastic indentations, relationships between *P*, *h*, *a*, and *S* are readily derivable in numerical form. More details on the calculation have been published elsewhere [17, 19]. A free solver written for MATLAB® is available on the archival website iMechanica [26].

Figure 1(a) shows the relationship between the contact stiffness *S* and the contact radius *a* for different values of the film/substrate elastic mismatch and for several indenter geometries. Both conical punches with different apex angles and spherical punches of different radii are considered. Here *S* is normalized by the product of M_s and film thickness *t*, and *a* is normalized by *t*. Clearly, the *S*-*a* relationship does not depend on indenter geometry; it depends solely on the elastic properties of film and substrate. This is a well-known result for bulk indentation of monolithic materials [27] that is recovered here for the case of a layered medium. Because the *S*-*a* relationship is independent of indenter geometry, one can define an effective indentation modulus for the film/substrate system as $M_{eff} = S\sqrt{\pi}/2\sqrt{A} = S/2a$. In general, the effective modulus is a function of indentation depth. For indentation of a homogeneous material, it reduces to the plane-strain modulus of the material. In Figure 1(b), we compare the effective modulus obtained from Yu's analysis with finite element calculations reported by Gao [20] and by Sakai [28]. Very good agreement is achieved, giving confidence in both the numerical solution of the integral equation and the finite element calculations.

III. APPLICATION A: ELASTIC INDENTATIONS ON EPITAXIAL FILMS

When analyzing indentation experiments in epitaxial films, one needs to take into account that the film and/or substrate are very often elastically anisotropic; solutions including Yu's

solution for isotropic materials are not immediately applicable. First consider a monolithic crystal with a three- or four-fold rotational axes perpendicular to its surface. Examples include cubic single crystals with their surface parallel to the (100) or the (111) plane, and hexagonal crystals with their surface parallel to the basal plane. It was shown by Vlassak and Nix [29, 30] that the contact area between an axisymmetric indenter and such a crystal is exactly circular. Therefore, the indentation modulus defined as $M = S\sqrt{\pi}/2\sqrt{A} = S/2a$ is consistent with the isotropic case. The elastic indentation response of the crystal is identical to that of an isotropic material with the same indentation modulus. Using the appropriate definition of the indentation modulus and the concept of equivalent isotropic solution, this approach can be further extended to crystals with arbitrary orientation as discussed by Vlassak et al in [31].

A rigorous solution for the elastic indentation of an anisotropic film on an anisotropic substrate is not readily available. Instead we propose to use Yu's isotropic solution, where we replace the anisotropic materials with equivalent isotropic materials that have the same elastic indentation behavior. Specifically, we require that the corresponding material have a plane-strain modulus and Poisson's ratio identical to the indentation modulus and average anisotropic Poisson's ratio of the original material. The assumption here is that the depth-dependence of the indentation response is similar for isotropic and anisotropic materials. To substantiate this assumption, figures 2(a) through 2(c) show the indentation loads, the contact stiffnesses, and the effective indentation moduli versus indentation depth for several (100)-oriented metallic films on (100)-silicon substrates, calculated using both finite elements and the modified Yu solution. A Berkovich-equivalent conical tip is considered. The material parameters used in the calculations are listed in table 1. Evidently, the results from the modified Yu solution are in good agreement with those obtained from the anisotropic FEM simulations, although the modified Yu solution yields more accurate results for very shallow indentations. Note that the Poisson's ratios of film and substrate have only minimal effect on the results [19], and the values used are those for the

random polycrystalline aggregates [32].

We use the modified Yu solution to analyze elastic indentations of epitaxial gold films grown on (100)-oriented single-crystal sodium chloride substrates. The indentation experiments were performed by Dietiker and colleagues as reported in [33]. The gold film thickness ranged from 68 nm to 858 nm. The indentation tests were carried out in load-control mode using a blunt Berkovich indenter with an indenter tip radius of approximately 700 nm as determined by atomic force microscopy (AFM). A simple method for calculating the indentation modulus for a crystal with arbitrary symmetry has been provided by Vlassak and Nix [29]. Table 1 lists the corresponding values of the indentation moduli for sodium chloride and gold calculated using the elastic constants from [33].

Figure 3 shows the experimental *P*-*h* data reproduced from figure 3(b) in [33]. For clarity, the starting points of the curves have been shifted. All films undergo reversible elastic deformation before the first pop-in event, which occurs at an indentation depth of approximately 6 to 7 nm and indicates incipient plasticity. We note that a substrate effect in these measurements cannot be ruled out *a priori* for two reasons: (1) the indentation contact radii are significant compared to the thicknesses of the films, and (2) gold is stiffer than sodium chloride making the indentation response more sensitive to the presence of the substrate [12]. Figure 3 shows the best fit of Yu's solution (solid curves) to the elastic portions of the experimental *P*-*h* curves, where we have used Yu's solution for a spherical tip because the experimental indentation depths are small compared to the tip curvature. The indentation moduli of the films were taken as the sole fitting parameters in this procedure; the indentation modulus of the substrate was set to the experimental value measured in [33]. It is evident from the figure that the modified Yu's solution provides a very good description for the elastic portions of the indentation curves. The indentation moduli of the gold films determined from the fits are listed in table 2, along with the values obtained if the substrate effect is ignored. The indentation moduli obtained using Yu's solution show little variation with film thickness. Only the thinnest film has a modulus that is approximately 10%

lower than that of the other films, possibly caused by an increased fraction of micro-voids in the film [33, 34]. If, by contrast, the substrate effect is ignored and the films are treated as monolithic, there is a strong apparent variation with film thickness [33]. Clearly substrate effects need to be accounted for, even if the indentation depth is significantly less than 10% of the film thickness. This is especially so if the substrate is more compliant than the film. The effect is illustrated graphically in the inset of figure 3, which plots load as a function of indentation depth for gold films of different thicknesses. The load is normalized by the load that would be required to indent a monolithic gold film to the same depth. It is obvious from the figure that the substrate effect is not negligible even for the thickest film at shallow depths.

Finally it should be noted that pyramidal indenters are used in many experiments. It was shown that the indentation modulus obtained for a triangular contact is related to that for a circular contact by a correction factor close to unity and that the effect of the in-plane orientation of the indenter on an anisotropic surface is very small even for materials with very large anisotropy [29]. These statements imply that the approach proposed in this paper can also be used for these commonly used indenters.

IV. APPLICATION B: ELASTO-PLASTIC INDENTATIONS WITH SIGNIFICANT PILE-UP

The second application of Yu's solution is for elasto-plastic materials where indentation pile-up is significant. In an elasto-plastic indentation, the process of unloading from a hardness impression can be modeled as an elastic contact between a flat surface and an effective indenter [35]. Although the shape of the effective indenter depends on the elastic and plastic properties of the indented materials and is usually unknown, the relationship between contact stiffness S and contact radius a, which is independent of the precise indenter shape, can still be calculated. The same argument is valid when the indentation is performed on a film/substrate composite, as long as the presence of the substrate is taken into account in the elastic analysis [19]. Chen and

Vlassak modeled the elasto-plastic indentation of a film on a substrate with finite elements [12]. They demonstrated that the elastic unloading process was well approximated by Yu's elastic contact solution, which provided a unique relationship between *S* and *a*, even in the presence of significant plastic pile-up. This shape-independent *S*-*a* relation was later adopted by Han et al to determine the hardness of a thin film on an elastically mismatched substrate [17]. In Han's method, the contact stiffness was measured experimentally and the contact area was then estimated using the *S*-*a* relation derived from Yu's solution. This method was demonstrated to yield accurate results, but required that the elastic constants of both the film and the substrate be known *a priori*. In a recent paper [19], Li and Vlassak reported on a method for analyzing indentation experiments that combines Yu's solution with the classic Oliver and Pharr approach [1]. This method does not require knowledge of the elastic constants of the film and works well as long as there is little plastic pile-up around the indenter. Here we extend this method to materials that do pile up significantly. In this case, the contact area between the indenter and the film needs to be measured independently using AFM or another suitable technique [5-9].

Before we describe the analysis procedure, we need to emphasize an important practical difference between the analysis of elastic and elasto-plastic indentations using Yu's solution as follows. In an elastic indentation, the film thickness is well defined and application of the Yu solution is relatively straightforward. In elasto-plastic indentations, however, the film between indenter and substrate is thinned as a result of plastic flow and it is not immediately clear what thickness should be used. Saha and Nix [11] used the initial film thickness subtracted by the indentation depth, $t-h$, whereas Han et al [17] simply used t. In a previous report [19], we showed that the local thinning effect is well captured if an effective film thickness, t_{eff}, is defined as

$$t_{eff} = t - \eta \cdot h \tag{2}$$

where the dimensionless parameter η quantifies the local thinning of the film caused by plastic

flow in the film. This parameter depends on the mechanical properties of film and substrate, as well as on the shape of the indenter. Preliminary finite element calculations show that η is nearly independent of indentation depth and that its value ranges from 0.3 to 0.7 for materials that do not work harden.

We propose the following procedure for analyzing indentation experiments in films that show significant pile-up. At a given indentation depth, the contact area A is measured using a technique such as AFM. Here the equivalent contact radius $a = \sqrt{A/\pi}$ is referred to as the experimental contact radius a^{exp}. The contact radius at this position can also be calculated from the S-a relationship derived from Yu's solution, if the values of η and the plane-strain modulus of the film, M_f, are assumed. The elastic S-a relation (as in figure 1) then yields a contact radius value that corresponds to the instantaneous contact stiffness S and that we call the theoretical contact radius a^{th}.

If a series of indentations are made to different depths, a sequence of (a^{exp}, a^{th}) pairs, one for each indentation, is obtained. If the assumed values of η and M_f are correct, a^{exp} should equal to a^{th} for all depths. In actual practice, η and M_f are not known and they can be treated as free parameters to obtain the best possible agreement between a^{exp} and a^{th}. The degree of agreement can be quantified using the sum of the residues squared,

$$\chi^2 = \sum_i \left(a_i^{\text{exp}} - a_i^{th} \right)^2 , \tag{3}$$

where the sum runs over all the indentations. The last step is to find the pair (η, M_f) that minimizes χ^2 using a standard optimization algorithm. Note that the tip area calibration function is not needed in this analysis because the contact area between indenter and sample is measured directly.

We proceed to verify the proposed procedure using load-displacement data obtained both from finite element simulations and from indentation experiments. The indentations are simulated

using the commercial code ABAQUS 6.7. For simplicity, the indenter is modeled as a rigid cone with a half-apex angle of 70.3°. The film and substrate are modeled as elastic-perfectly plastic von Mises materials, and are meshed with 8-node axisymmetric elements. The boundary conditions, model size, and meshing are similar to [12]. Frictionless contact is assumed between the indenter and the film material. All simulations are performed with the large-strain capability of ABAQUS enabled. Input material properties are listed in table 3 that includes both stiff films on a compliant substrate (Film-1 series) and compliant films on a stiff substrate (Film-2 series). For each case, the yield strength of the film is also varied over a wide range. At several indentation depths, the contact stiffness is determined from an elastic unloading step using a power-law fit [1], and the contact radius a^{exp} is determined from the nodes in contact with the indenter. Figure 4(a) shows the results. The square symbols denote a^{exp} obtained directly from the FEM simulations; the circle symbols are the best-fitting a^{th} obtained from the Yu solution, where M_f and η were used as fitting parameters. Close agreement is obtained for all depths. The results are summarized in table 3. For example, the values of M_f and η obtained from the fit for Film-1-2 are 325.3±2.4 GPa and 0.40±0.01, respectively, where the uncertainties in M_f and η are the standard errors of the parameters. The extracted value of M_f deviates less than 1.7% from the FEM input value. Similar accuracy is obtained for all material systems simulated in this study: the indentation moduli of the films deviate less than 4% from the input values over a wide range of film properties.

For the indentation experiments, 1 μm copper films were deposited on (100)-silicon and fused silica substrates. The films were deposited using a direct-current magnetron sputter system with a high-purity copper target (99.999%) and a base pressure of 8×10^{-8} Torr. The depositions were performed at a DC power of 200W and with an Ar working gas pressure of 5×10^{-3} Torr. Immediately prior to the deposition, the substrates were sputter-cleaned for 5 minutes using Ar plasma. A thin titanium layer (~10 nm) was deposited to enhance the adhesion of the copper films.

To minimize oxidation, the samples were kept in vacuum before testing. All nanoindentation tests were conducted in load-control mode using a calibrated Ultra Nanoindentation Tester (CSM Instruments, Switzerland) equipped with a diamond Berkovich tip. Thermal drift during indentation experiments has been demonstrated to be negligible for this system [36]. The indentation loading scheme was similar for all tests: the measurements started with increasing the load at constant rate until a specified peak value was reached in 10 seconds. The load was held constant for 60 seconds followed by a fast unloading at a constant rate. The duration of the hold and the unloading rate were selected to minimize the error introduced by time-dependent deformation during unloading according to the method proposed in ref. [37]. Peak loads were varied such that the corresponding indentation depths were spaced evenly from approximately 10% to 90% of the film thickness for 9 different depths. The measurement was repeated ten times for each depth, and the results are the average of each group. After the indentation tests, 2 to 4 indentations in each group were examined with an integrated high-resolution atomic force microscopy (AFM). The lateral magnification of the AFM was calibrated using a standard step sample. The projected area of contact was measured using the differentiated height profile, which provides a sharper contact contour than the regular height profile. The indentation moduli of the substrates were determined from indentation measurements on the bare substrates. Figure 4(b) shows the experimental results along with the best fit of the *S*-*a* relationship. Standard corrections for finite tip compliance and for non-axisymmetric tip shape were applied in the analysis of the experiments [2, 29]. The results are summarized in table 4. The values of M_f obtained from Yu's solution are 136.8 ± 1.7 GPa and 142.1 ± 1.3 GPa for the Cu-1 and Cu-2 films, respectively. The corresponding values of η are 0.44 ± 0.02 and 0.42 ± 0.03. Even though indentations up to 90% of the film thickness were used in the analysis, the indentation moduli for the Cu-1 and Cu-2 films are in good agreement with each other, as well as with experimental values for bulk copper in the literature [38]. Evidently, the analysis is successful at eliminating the effect of the substrate.

V. CONCLUSIONS

In summary, we have shown how Yu's solution for the elastic indentation of a layered half-space can be used to analyze indentation experiments where substrate effects are important. Two cases are considered: elastic indentations where film and substrate are anisotropic and elasto-plastic indentations with significant material pile-up. In both cases, experiments and finite element simulations show that elastic substrate effects can be eliminated through use of Yu's solution, even if there is significant elastic mismatch between film and substrate. Thus it is possible to obtain intrinsic properties for very thin films with current indentation technology.

ACKNOWLEDGEMENTS

The authors would like to acknowledge Rahul Nair from CSM Instruments for the nanoindentation and AFM measurement. HL and JJV acknowledge support from the National Science Foundation (NSF) under Grant CMS-0556169.

REFERENCES

1. Oliver, W.C. and G.M. Pharr, *An Improved Technique for Determining Hardness and Elastic-Modulus Using Load and Displacement Sensing Indentation Experiments.* Journal of Materials Research, 1992. **7**(6): p. 1564-1583.
2. Oliver, W.C. and G.M. Pharr, *Measurement of hardness and elastic modulus by instrumented indentation: Advances in understanding and refinements to methodology.* Journal of Materials Research, 2004. **19**(1): p. 3-20.
3. Fischer-Cripps, A.C., *Nanoindentation*. 2 ed. 2004: Springer Verlag.
4. Pharr, G.M., *Measurement of mechanical properties by ultra-low load indentation.* Materials Science and Engineering a-Structural Materials Properties Microstructure and Processing, 1998. **253**(1-2): p. 151-159.
5. Randall, N.X., C. Julia-Schmutz, and J.M. Soro, *Combining scanning force microscopy with nanoindentation for more complete characterisation of bulk and coated materials.* Surface & Coating Technology 1998. **108**(1-3): p. 489-495.
6. Randall, N.X., *Direct measurement of residual contact area and volume during the nanoindentation of coated materials as an alternative method of calculating hardness.* Philosophical Magazine A-Physics of Condensed Matter Structure Defects and Mechanical Properties, 2002. **82**(0): p. 1883-1892.
7. Lim, Y.Y., M.M. Chaudhri, and Y. Enomoto, *Accurate determination of the mechanical properties of thin aluminum films deposited on sapphire flats using nanoindentations.* Journal of Materials Research, 1999. **14**(6): p. 2314-2327.
8. Sakai, M., N. Hakiri, and T. Miyajima, *Instrumented indentation microscope: A powerful tool for the mechanical characterization in microscales.* Journal of Materials Research, 2006. **21**(9): p. 2298-2303.
9. Fang, L., et al., *Continuous electrical in situ contact area measurement during instrumented indentation.* Journal of Materials Research, 2008. **23**(9): p. 2480-2485.
10. Gao, H.J., C.H. Chiu, and J. Lee, *Elastic Contact versus Indentation Modeling of Multilayered Materials.* International Journal of Solids and Structures, 1992. **29**(20): p. 2471-2492.
11. Saha, R. and W.D. Nix, *Effects of the substrate on the determination of thin film mechanical properties by nanoindentation.* Acta Materialia, 2002. **50**(1): p. 23-38.
12. Chen, X. and J.J. Vlassak, *Numerical Study on the Measurement of Thin Film Mechanical Properties by Means of Nanoindentation.* Journal of Materials Research, 2001. **16**(10): p. 2974-2982.
13. Mencik, J., et al., *Determination of elastic modulus of thin layers using nanoindentation.* Journal of Materials Research, 1997. **12**(9): p. 2475-2484.
14. Pharr, G.M. and W.C. Oliver, *Measurement of thin-film mechanical properties using nanoindentation.* MRS Bulletin, 1992. **17**(7): p. 28-33.
15. King, R.B., *Elastic Analysis of Some Punch Problems for a Layered Medium.* International Journal of Solids and Structures, 1987. **23**(12): p. 1657-1664.
16. Yu, H.Y., S.C. Sanday, and B.B. Rath, *The Effect of Substrate on the Elastic Properties of Films Determined by the Indentation Test - Axisymmetrical Boussinesq Problem.* Journal of the Mechanics and Physics of Solids, 1990. **38**(6): p. 745-764.
17. Han, S.M., R. Saha, and W.D. Nix, *Determining hardness of thin films in elastically mismatched film-on-substrate systems using nanoindentation.* Acta Materialia, 2006. **54**(6): p. 1571-1581.
18. Tsui, T.Y. and G.M. Pharr, *Substrate effects on nanoindentation mechanical property measurement of soft films on hard substrates.* Journal of Materials Research, 1999. **14**(1): p. 292-301.

19. Li, H. and J. Vlassak, *Determining the elastic modulus and hardness of an ultra-thin film on a substrate using nanoindentation.* Journal of Materials Research, 2009. **24**(3): p. 1114-1126.
20. Gao, Y.F., et al., *Effective elastic modulus of film-on-substrate systems under normal and tangential contact.* Journal of the Mechanics and Physics of Solids, 2008. **56**(2): p. 402-416.
21. Bhattacharya, A.K. and W.D. Nix, *Analysis of elastic and plastic-deformation associated with indentation testing of thin-films on substrates.* International Journal of Solids and Structures, 1988. **24**(12): p. 1287-1298.
22. Bull, S.J., *Nano-indentation of coatings.* Journal of Physics D-Applied Physics, 2005. **38**(24): p. R393-R413.
23. Fischer-Cripps, A.C., *Review of analysis and interpretation of nanoindentation test data.* Surface & Coatings Technology, 2006. **200**(14-15): p. 4153-4165.
24. Sneddon, I.N., *The relation between load and penetration in the axisymmetric Boussinesq problem for a punch of arbitrary profile.* International Journal of Engineering Science, 1965 **3**: p. 47.
25. Elgendi, S.E., *Chebyshev Solution of Differential, Integral and Integro-Differential Equations.* Computer Journal, 1969. **12**(3): p. 282-&.
26. *url: http://imechanica.org/node/4050. "iMechanica" is a website hosted at the Harvard School of Engineering and Applied Sciences dedicated to enhancing communication and discussion among mechanicians*
27. Pharr, G.M., W.C. Oliver, and F.R. Brotzen, *On the generality of the relationship among contact stiffness, contact area, and elastic-modulus during indentation* Journal of Materials Research, 1992. **7**(3): p. 613-617.
28. Sakai, M., *Substrate-affected indentation contact parameters of elastoplastic coating/substrate composites* Journal of Materials Research, 2009. **24**(3): p. 831-843.
29. Vlassak, J.J. and W.D. Nix, *Measuring the Elastic Properties of Anisotropic Materials by Means of Indentation Experiments.* Journal of the Mechanics and Physics of Solids, 1994. **42**(8): p. 1223-1245.
30. Vlassak, J.J. and W.D. Nix, *Indentation Modulus of Elastically Anisotropic Half-Spaces.* Philosophical Magazine a-Physics of Condensed Matter Structure Defects and Mechanical Properties, 1993. **67**(5): p. 1045-1056.
31. Vlassak, J.J., et al., *The indentation modulus of elastically anisotropic materials for indenters of arbitrary shape.* Journal of the Mechanics and Physics of Solids, 2003. **51**(9): p. 1701-1721.
32. Vlassak, J.J., *New experimental techniques and analysis methods for the study of the mechanical properties of materials in small volumes*, in *Department of Materials Science and Engineering*. 1994, Stanford University.
33. Dietiker, M., et al., *Nanoindentation of single-crystalline gold thin films: Correlating hardness and the onset of plasticity.* Acta Materialia, 2008. **56**(15): p. 3887-3899.
34. Gruber, P.A., et al., *Strong single-crystalline Au films tested by a new synchrotron technique.* Acta Materialia, 2008. **56**(8): p. 1876-1889.
35. Pharr, G.M. and A. Bolshakov, *Understanding nanoindentation unloading curves.* Journal of Materials Research, 2002. **17**(10): p. 2660-2671.
36. Nohava, J., N.X. Randall, and N. Conte, *Novel ultra nanoindentation method with extremely low thermal drift: Principle and experimental results.* Journal of Materials Research, 2009. **24**(3): p. 873-882.
37. Feng, G. and A.H.W. Ngan, *Effects of creep and thermal drift on modulus measurement using depth-sensing indentation.* Journal of Materials Research, 2002. **17**(3): p. 660-668.
38. McElhaney, K.W., J.J. Vlassak, and W.D. Nix, *Determination of indenter tip geometry and indentation contact area for depth-sensing indentation experiments.*

Journal of Materials Research, 1998. **13**(5): p. 1300-1306.
39. Brantley, W.A., *Calculated Elastic-Constants for Stress Problems Associated with Semiconductor Devices.* Journal of Applied Physics, 1973. **44**(1): p. 534-535.

Tables

Table 1. Single-crystal elastic constants and indentation moduli

Material	c_{11} (GPa)	c_{12} (GPa)	c_{44}(GPa)	Poisson's ratio [a]	Indentation modulus on (100) plane(GPa)
NaCl [33]	49.4	12.8	12.7	0.25	41.0 (theoretical), 44.5[b] (experimental [33])
Au [33]	193	164	41.5	0.43	90.2 (theoretical)
Cu [32]	170.2	114.9	61.0	0.35	129.0 (theoretical)
Si [39]	165.7	63.9	79.56	0.22	164.8(theoretical)
W [32]	522.4	204.4	160.8	0.28	442.0 (theoretical)

[a] Value for a polycrystal with random texture, calculated following [32].

[b] This value is used in the calculation.

Table 2. Experimental data from [33]

Gold film thickness (nm):		858	429	207	134	68
Indentation modulus (GPa)	This study using Yu's solution	100.6±4.3	101.5±5.1	98.3±3.7	97.9±2.9	89.0±7.4
	From [33], calculated using equation for a monolithic material	109.1	91.8	79.4	65.7	57.0

Table 3. Summary of material properties in the FEM simulations

Material	Input Young's modulus (GPa)	Poisson's ratio	Input M_f (GPa)	Yield stress (GPa)	Calculated M_f (GPa)	η
Film-1-1[a]	300	0.25	320	0.2	314.7±3.2	0.41±0.02
Film-1-2				1	325.3±2.4	0.40±0.01
Film-1-3				5	309.3±4.1	0.30±0.02
Film-2-1	33.3	0.25	35.6	0.2	34.7±0.6	0.34±0.03
Film-2-2				1	34.2±0.9	0.35±0.01
Film-2-3				5	36.3±0.8	0.39±0.01
Substrate	100	0.25	106.7	1	-	-

[a] All films are 1 μm thick.

Table 4. Summary of experimental data and results of copper films

Material	Poisson's ratio [a]	Film thickness (μm)	Indentation modulus (GPa)	η
Cu-1	0.35	1.084±0.006	136.8±1.7	0.44±0.02
(100)-Si, substrate for Cu-1	0.22	-	173.2[b]	-
Cu-2	0.35	1.064±0.005	142.1±1.3	0.42±0.03
fused silica, substrate for Cu-2	0.17	-	75.2[b]	-

[a] Literature values [14, 17, 32].
[b] Determined experimentally.

Figures

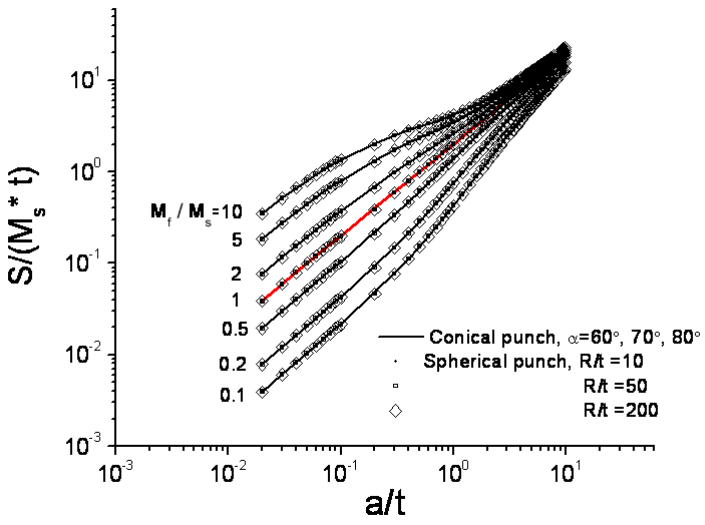

Figure 1(a)

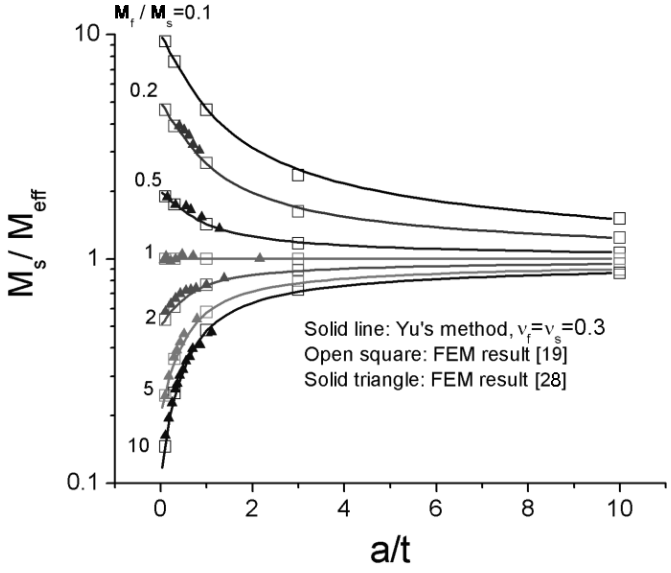

Figure 1(b)

Figure 1. (a) Normalized contact stiffness as a function of normalized contact radius for film/substrate composites with different elastic mismatch and for different indenter shapes [19]. (b) Comparison of the effective indentation moduli derived from Yu's solution and from elastic finite element calculations [20, 28].

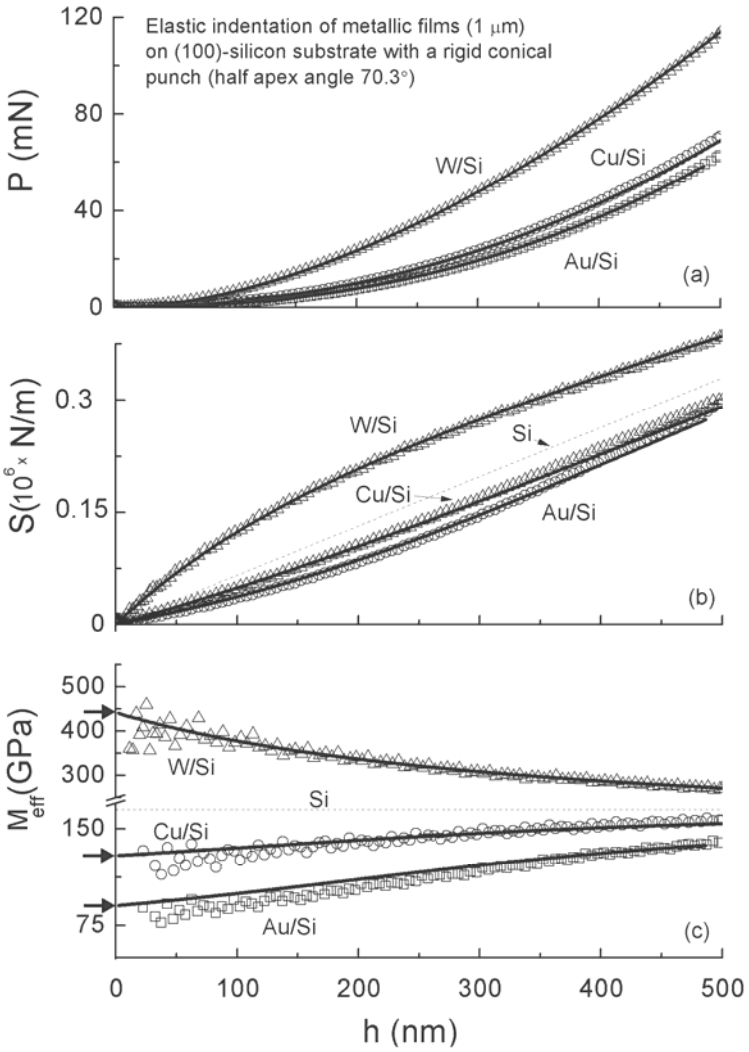

Figure 2. Comparison of (a) indentation load, (b) contact stiffness, and (c) effective indentation moduli as a function of indentation depth calculated from anisotropic FEM simulations (markers) and from Yu's elastic solution (solid curves). Arrows indicate the theoretical indentation moduli of the film materials.

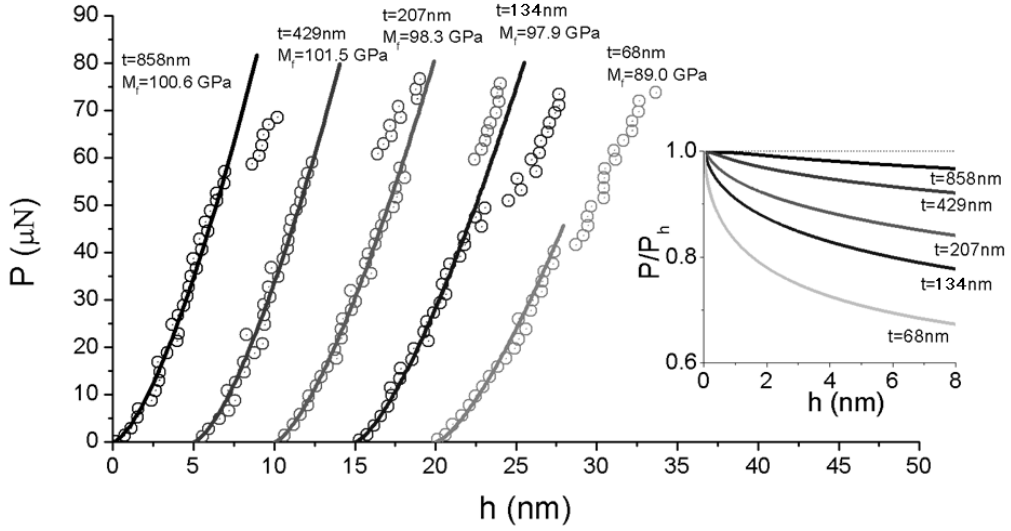

Figure 3. Comparison of the load-displacement curves for gold films of various thicknesses on sodium chloride substrates. The circular markers are experimental data from [33]; the solid curves are based on Yu's elastic solution. Origins of the data sets have been shifted for clarity. The inset shows the deviation of the indentation response from the monolithic contact model due to the substrate effect; film moduli are the same. Tip radius (700nm) and elastic properties of the substrate (M_s = 44.5GPa, ν_s = 0.25) are taken as experimentally determined in [33].

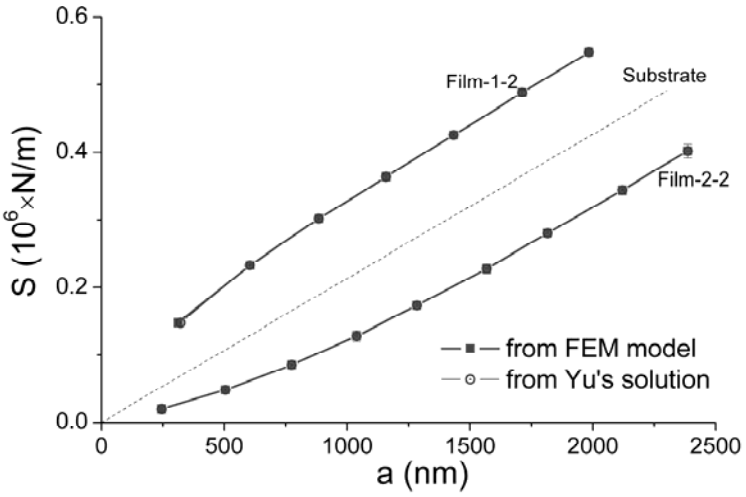

Figure 4(a)

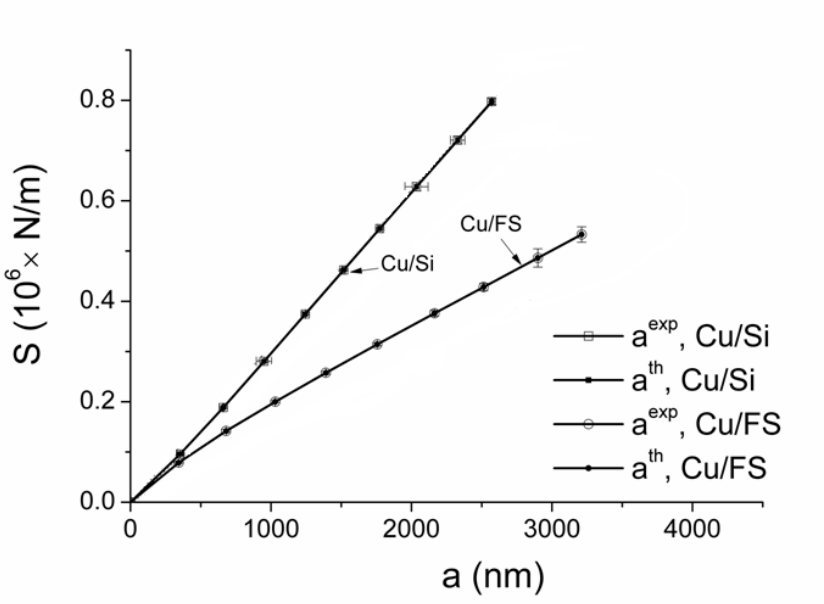

Figure 4(b)

Figure 4. Comparison of the experimental and theoretical estimations of the *S*-*a* relation for (a) finite element simulations (Film-1-2 and Film-2-2), and for (b) indentation experiments on Cu films on silicon and fused silica (FS) substrates.